



## Dynamic Performance of Small Sized Lead Rubber Bearings for Nuclear Equipment

Tae-Myung Shin<sup>1\*</sup>, Gyeong-Hoi Koo<sup>2</sup>

<sup>1</sup> Korea National University of Transportation, Chungju 27469, Korea

<sup>2</sup> Korea Atomic Energy Research Institute, Daejeon 34057, Korea

\* [tmshin@ut.ac.kr](mailto:tmshin@ut.ac.kr) (Corresponding Author)

### ABSTRACT

The paper describes the development and testing of a small-sized lead rubber bearing (LRB) designed to enhance the seismic performance of mechanical or electrical equipment in Korean operating nuclear power plants against beyond design basis earthquakes (BDBEs). Challenges are faced in designing a small-sized LRB for relatively light equipment due to the difficulties of forming thin rubber sheets into small laminated structures. After considering different design options with varying vertical load capacities, a 1-ton LRB is chosen as the most optimal design type based on static shear performance tests and stability reviews. After repeated design, fabrication, and static test feedback for optimization and added a lead core to increase the damping capacity. And Seismic analyses of an isolated system model are conducted to ensure that the LRB demonstrated the desired dynamic characteristics and seismic performance. Verification tests using a three-dimensional vibration table are performed to investigate the seismic capacity of the LRB. The seismic responses of the table and isolated dummy mass are measured and compared to assess the LRB's performance for both primary and secondary structures in the concerning frequency range of BDBEs. The results showed that the small-sized 1-ton capacity LRB behaved satisfactorily in terms of seismic performance for both primary and secondary structures within the frequency range of BDBEs

### INTRODUCTION

The earthquakes in Gyeongju and Pohang in 2016 caused public concerns about the safety of nuclear power plants and their ability to withstand seismic events, particularly beyond design basis earthquakes (DBEs). If an earthquake occurs that is greater than the design level for a structure installed in a nuclear power plant, it is important to assess the actual performance of the structure and determine if the design margin is sufficient. This assessment can be done through various types of analyses, such as seismic hazard analysis, structural analysis, and dynamic analysis. If it is found that the structure's seismic performance is insufficient, then steps should be taken to improve it. This may involve retrofitting or upgrading the structure with new seismic safety features or components, such as small-sized LRBs, to improve its seismic performance and enhance its ability to withstand future earthquakes. In the case of operating nuclear power plants, it may be more efficient to use equipment isolation rather than building isolation to enhance the seismic safety of the facility [1-3]. The equipment can be pressure vessels, pumps, electric control cabinets, emergency diesel generator and etc. By the way, special design conditions are required to use the LRB for the seismic isolation since the nuclear facility components are relatively light and mainly installed at a high elevation from a ground. Especially, when applied to the components located at high elevations, the LRB should be designed to be horizontally flexible enough to make a frequency shift function, and to be stable enough to accommodate the large shear deformation by the amplified severe seismic loads at component supports [4-6].

This study is about the development of a small LRB in order to improve seismic performance to small facilities or devices in nuclear power plants. Until now, there have been many studies on medium-to-large seismic isolation bearings such as buildings or bridges, but LRB studies for small structures are lacking [7-9]. In particular, development research for application to safety-related major facilities or devices in nuclear power plants is extremely rare. In the study, LRB with unit capacity of 1 ton or more as a seismic isolator for small equipment has been designed, and static and dynamic performance tests were conducted according to the according to the guidelines [9,10,15], to ensure its seismic performance. This could potentially be used as an alternative for improving or reinforcing the seismic performance of safety-related devices in operating nuclear power plants for BDBE in the future.

## DESIGN OF SMALL LRB

### Background and design considerations

In general, the LRB is designed for seismic isolation of large structures like building or bridges against ground earthquakes. In the normal design of LRB, main parameters to be considered should be rubber material properties, vertical weight, isolation frequency, damping, and horizontal deformation for the target earthquake. However, the small-sized LRB for equipment isolation must be designed to accommodate severely amplified seismic excitation at the floor level, where they are installed. Therefore, the small-sized LRB must be fundamentally designed to assure the horizontal deformation stability as well as the seismic isolation performance due to the limitation of the total rubber height [2].

Two types of design option, OPT-1 and OPT-2, of a lead inserted LRB were designed in the early stage as shown in Figure 1. Here, OPT-1 design focuses on lowering the seismic isolation frequency but sacrifices the shape factors more than OPT-2 design. As such, it was expected that OPT-1 could reduce the acceleration seismic response but would result in much larger horizontal deformation of the LRB which was, inherently, a burden in the stability problem contained in a small-sized LRB design. On the other hand, the OPT-2 design focuses on the shape factors rather than the isolation frequency.

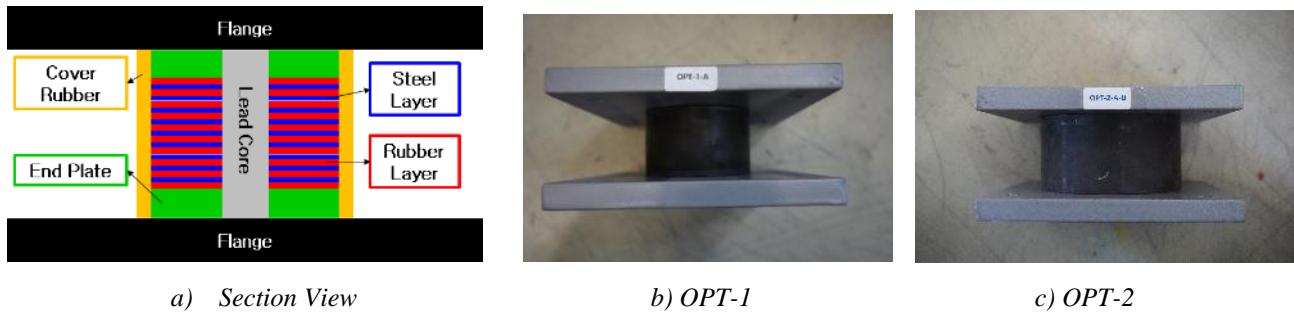


Figure 1. Shape of small LRB design options

Table 1. Design parameters of two LRB options

Properties	OPT1	OPT2
Design Load (ton)	1	1
Outer Diameter (mm)	76	100
Design Hori. Freq. (Hz)	<b>2.0</b>	<b>2.3</b>
Shape Factor, S1	7.6	9.9
Shape Factor, S2	4.4	5.0

Table 2. Mechanical properties of LRB materials

Material	Properties	Value
Rubber	Shear Modulus (MPa)	0.3
	Bulk Modulus (GPa)	1.96
	Tensile Strength (ksi)	2.5~3.5
	Density (g/cm <sup>3</sup> )	0.93
Lead	Shear Modulus (MPa)	8.33

### STATIC PERFORMANCE TEST

To verify the design specifications proposed in this paper as shown in Tables 1 and Table 2, the quasi-static mechanical property tests and the ultimate deformation tests were carried out. Figure 2 presents the schematics of the test machine used in this paper. The test equipment used for the static performance test to check the mechanical properties of LRB must satisfy the following conditions, and the contents are specified in ISO 22762-1[10].

Figure 2 shows a schematic diagram of the test machine, and No. 6 shown in the figure is the LRB corresponding to the prototype, and the vertical load is controlled through two vertical actuators, and the shear displacement is controlled through No. 5 horizontal actuators. Through this test, the load-displacement hysteresis curve can be checked, and the effective horizontal stiffness and damping ratio can be calculated using it. In addition, an LRB bi-linear model for LRB nonlinear model time history analysis can be derived. A total of three types of tests are performed: compression test, compression-shear test, and extreme behavior test. The vertical stiffness can be checked through the compression test, and the horizontal stiffness can be checked under the design surface pressure and transient surface pressure loading state through the compression-shear test. In addition, through the extreme behavior test, it is possible to visually check the destructive test of the prototype

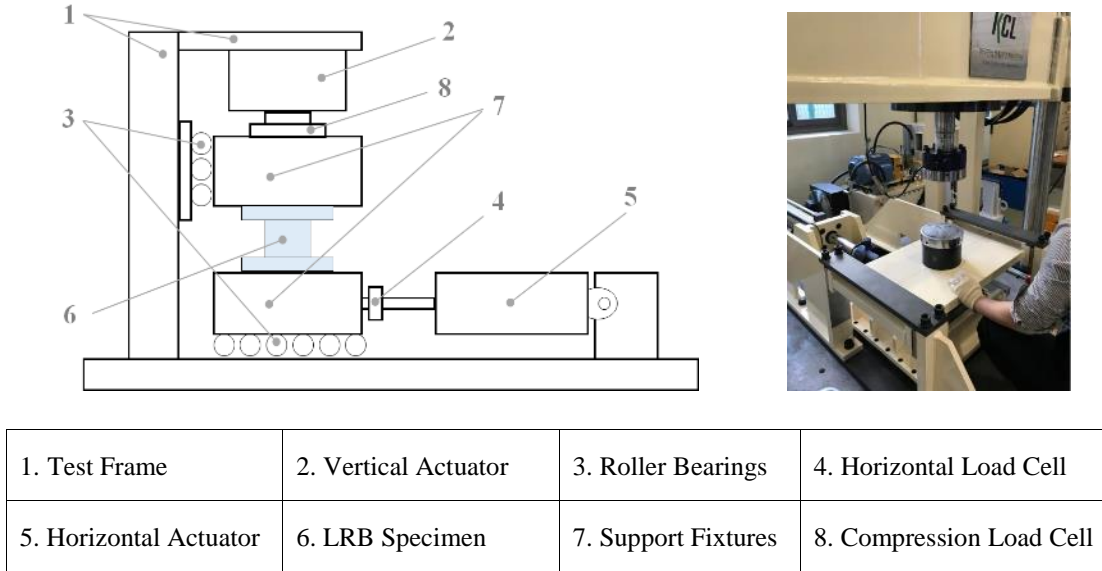


Figure 2. Schematics of quasi-static test facility

The static test of the small-sized LRB for equipment shows that the force-displacement response curve has hysteresis characteristics. It is similar to the typical shear deformation behaviour of the LRB for large structures until the shear strain reaches 300%. For the test data of the design shear deformation range ( $\pm 35$  mm: 200%) shown in Figure 3 and Figure 4, it presents the results of comparing the target design values with the tangential stiffness values. This result indicates that when the tangential stiffness curve was nonlinear, as shown in Figure 4, which was the actual test curve. The tangential stiffness, determined based on the half-position values of the design shear deformation, was highly volatile and was unreasonable to be a representative tangential stiffness.

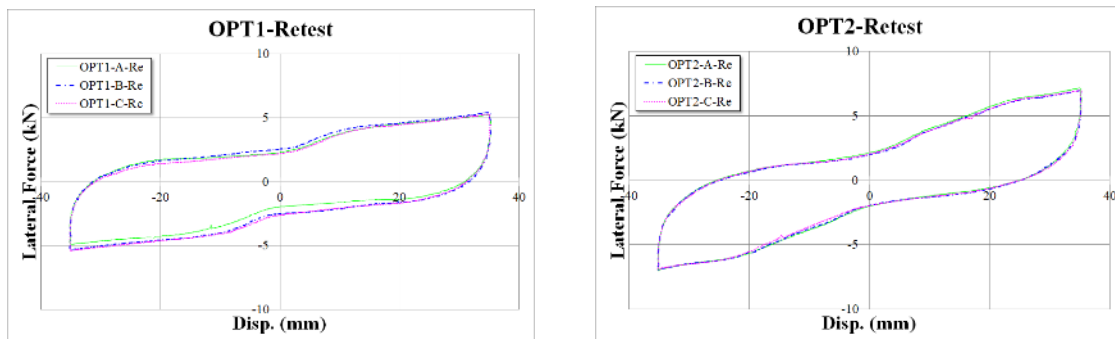


Figure 3. Static test results for design shear deformation range ( $\pm 35$  mm) of OPT-1 and OPT-2.

In order to confirm the characteristics of the LRB designed in this study, the effective horizontal stiffness value was derived from the compression-shear test results under the design conditions (vertical load 1ton, horizontal displacement 35 mm) and

compared with the design value. As a result of the compression-shear test of the prototype, it was confirmed that the effective horizontal stiffness showed a 10-15% error compared to the design value. The error range was within the  $\pm 20\%$  range suggested by the guideline.

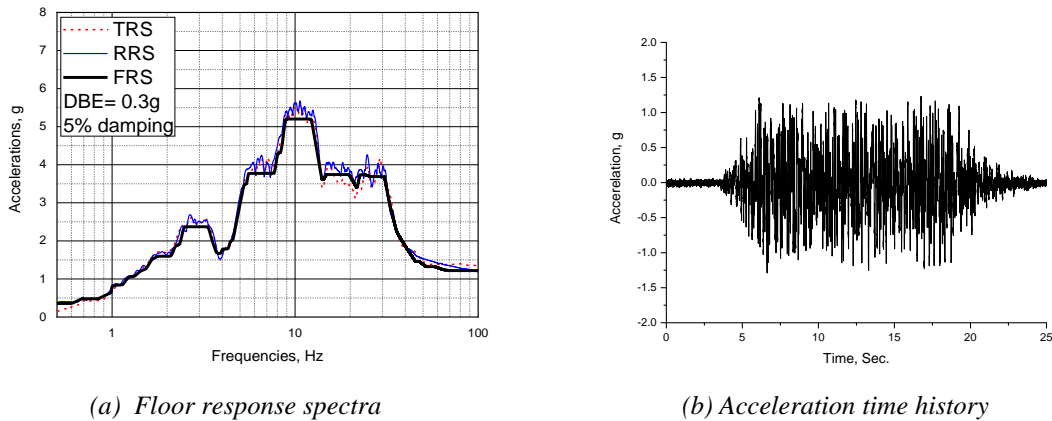


Figure 4. Shapes of LRB test and cross sections before and after the static tests

Figure 5 shows pictures of ultimate tests of 500% shear deformation and LRB sections for comparison before and after the test. As compared in the red circle area in the Figure 5, some of the steel sheets have shown too much plastic deformation in the edge side by the excessive shear and bending loads. However, in this case, it is interesting that the rubber maintained its overall shape and remain functional with no big cracks, which means still capable of isolating the seismic excitation before a total rupture. From the review of the quasi-static test and viewpoint of stability, OPT-1 has been chosen as a representative model.

### SIMULATION ANALYSIS FOR THE DYNAMIC TEST

Response spectrum analysis was conducted to evaluate the stress of the LRB for small facilities. The seismic inputs are acceleration floor response spectra (FRS) and time history at 137ft. level of plant structural model generated from 0.3g peak ground acceleration (PGA) of 5% damping, as shown in Figure 5. And it is also the design basis earthquake (DBE) of the reference plant. Analysis model was created as shown in Figure 5, and Figure 6 using ANSYS, a commercial program [16]. The finite element model for dynamic analysis was prepared in the same way as in the shaking table experiment, and as introduced in the previous section, it was supported by four seismic isolation bearings suitable for the capacity under the 4-ton dummy mass. The LRB model is a layered structure composed of steel and rubber plates, and was created as a three-dimensional solid element composed of a lead core in the center. As boundary conditions for the analysis, the lower parts of the LRB model were constrained. In addition, it was assumed that the lead core, each steel plate, and rubber plate are bonded.



(a) Floor response spectra

(b) Acceleration time history

Figure 5. Input seismic data (SSE 0.3g, 5% damping, 137ft).

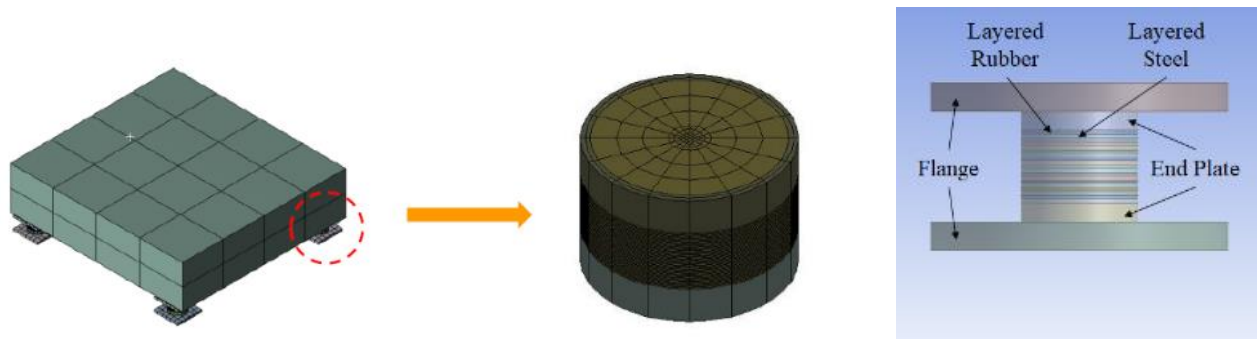


Figure 6. FEM Models of simulation analysis for dynamic Test

Table 3 show the analysis results for the maximum stresses of rubber and steel layers at three different seismic inputs of PGA of 0.4 g, 0.5 g, and 0.6 g, respectively. Rubber and steel can be roughly assumed to yield near the edge of the lead core at PGA 0.6 g, as depicted in Figure 7. Therefore, the maximum shear strength at the time of rubber failure is estimated using Hook's law at a shear modulus of 0.3-0.4 MPa, and according to the results of the previous study, it is about 1.8-2.4 MPa at a maximum shear strain of 600%, theoretically. Considering the results in Table 4 as reference values and shear strength estimates, it can be analytically inferred that local buckling or damage may have already started in the case of PGA 0.4g.

Table 3. Stress Analysis Results for Rubber and Steel Layers for BDBE

ZPA [g] of FRS (PGA)	Rubber Layer [MPa]	Steel Layer [MPa]
1.7(0.4)	3.9	437.4
2.2(0.5)	4.8	546.7
2.6(0.6)	5.8	656.0

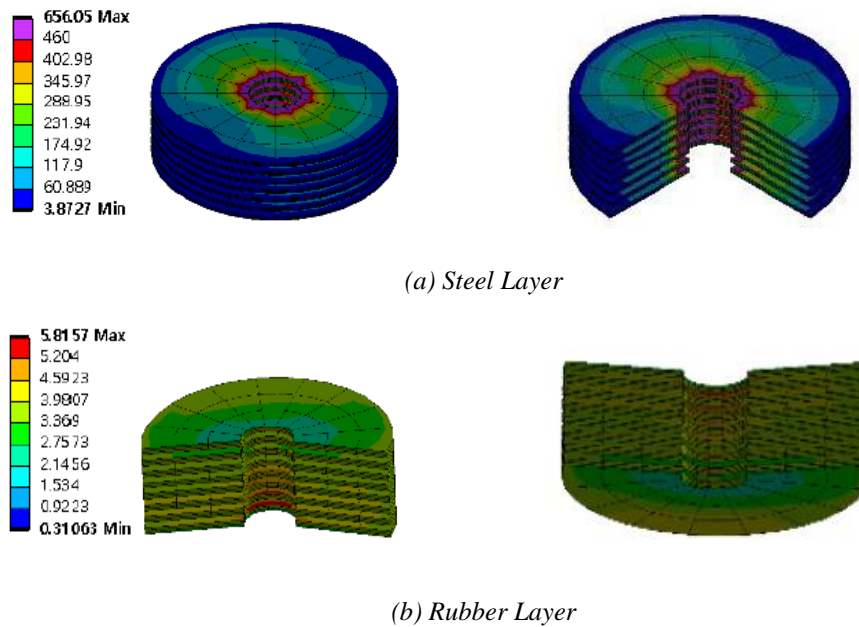


Figure 7. Stress distribution shapes in LRB for PGA 0.6g

**DYNAMIC TEST USING 3-AXIS SHAKING TABLE**

To investigate the dynamic characteristics of the small-sized LRB developed for an individual nuclear facility component seismic isolation, 3-axis shaking table test is performed. The technical specification of shaking table and test procedures are listed in Table 4. The sketch and picture of test model are shown in Figure 8. They consists of 4-ton dummy mass supported by 4 LRBs in the 4 corner bottoms and 2sets of 5Hz, 10Hz, 20Hz beams on the table and on top of the isolated mass. The beams are designed and installed to investigate seismic isolation effect on the secondary structures. The seismic inputs in the test are the same as used in simulation analysis.

Table 4. Shaking table specification and test procedures

Size[m]	4.0 x 4.0		
Max Loading (Force/Moment)	300 kN / 1,200kN-m		
Frequency Range(Hz)	0.1 ~ 60		
Control Axes	6 DOF		
Acceleration at Full Payload(g)	X	Y	Z
	1.2	1.2	0.8
Maximum Stroke(mm)	X	Y	Z
	±300	±200	±150

No.	LRB ID	ZPA of FRS (PGA)
1	OPT-2A	2.2g (0.5g)
2		1.3g (0.3g)
3		0.4g (0.1g)
4	OPT-2B	2.2g (0.5g)
5		1.3g (0.3g)
6		0.4g (0.1g)
7	OPT-2C	2.6g (0.6g)

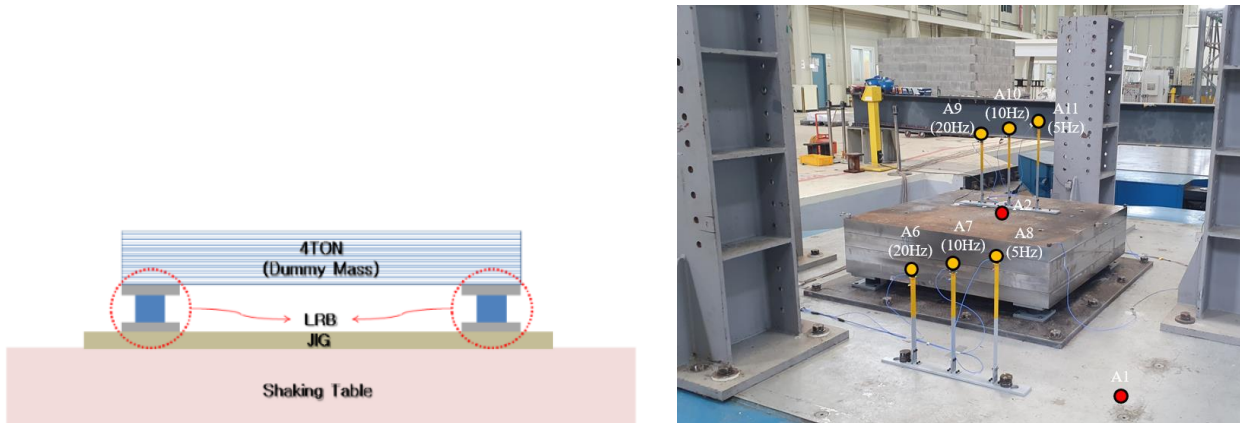


Figure 8. Schematics of 3D shaking table test

The test results for the representative design basis earthquake level of PGA = 0.3 g are presented in Figure 9. From the spectrum responses corresponding to the test results, we can see that the peak spectral frequency band around 10 Hz in the input shaking table motion is significantly shifted to the 2.6 Hz in the dummy mass response, which is slightly higher than the 2.3 Hz of the design seismic isolation frequency in Table 1. From the result, it can be confirmed that the LRB on development in this study has one of the typical seismic isolation characteristics that can assure the seismic isolation performance for the nuclear facility components generally having around 10 Hz dynamic frequencies. And the isolation effect on the secondary structures can be explained by comparison of the acceleration responses between the beams on the table and on the isolated mass. As shown in Figure 10, the isolation effect increase more and more as the natural frequency of the secondary structure becomes higher when compared between the three beams of 5Hz, 10Hz, 20 Hz natural frequency.

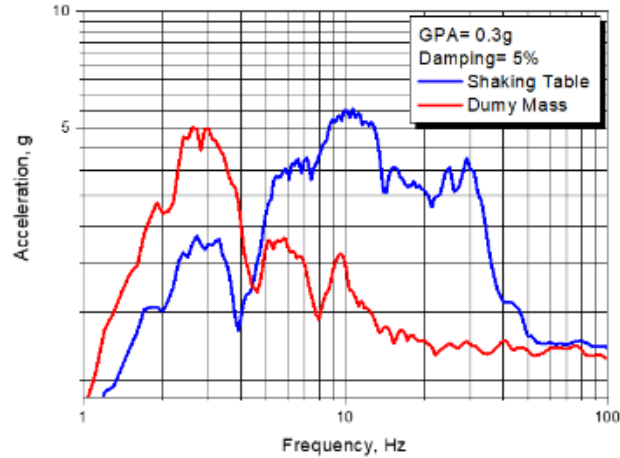


Figure 9. Isolation effect of dummy mass in acceleration response

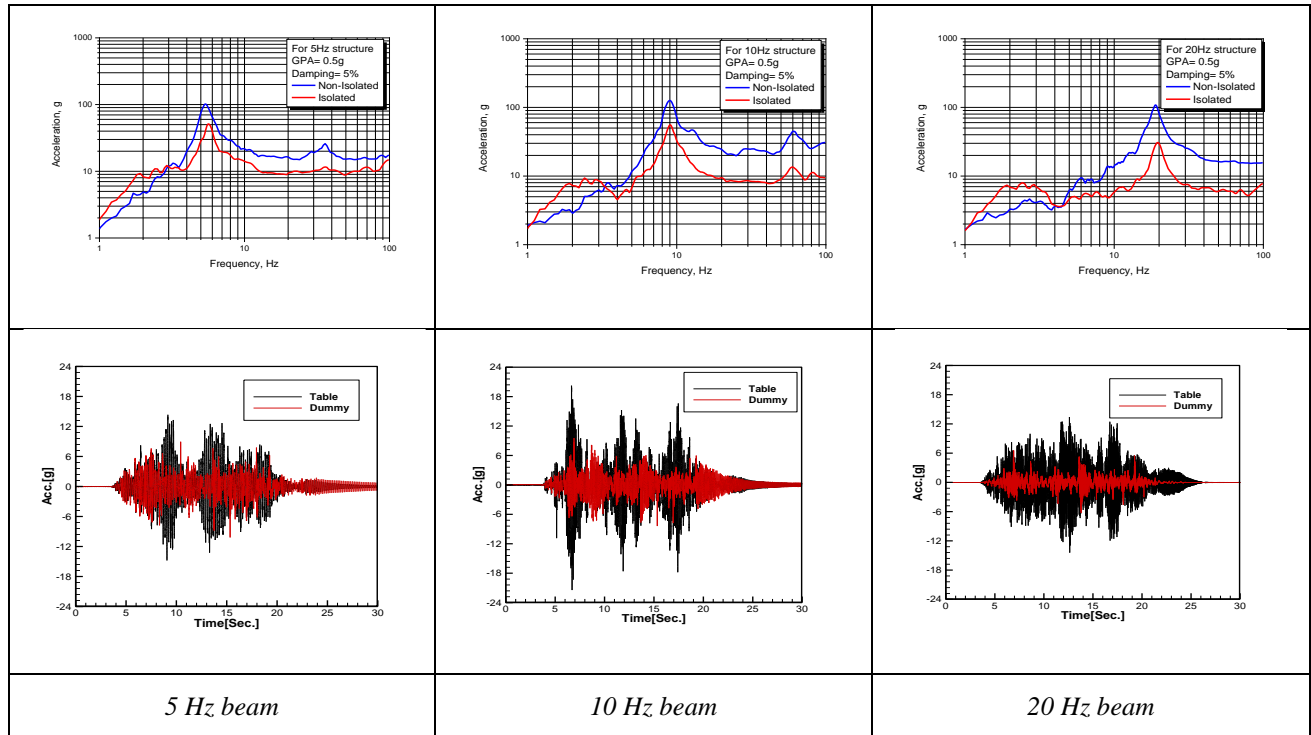


Figure 10. Acceleration response spectra and time history of 5Hz, 10Hz, 20Hz Beams by Isolation

### RESPONSE CHARACTERISTICS AFTER ISOLATION SYSTEM FAILURE

The model has passed through all the test procedure planned in Table 4 including 0.5g PGA test and remained safe. However, it failed during the 7<sup>th</sup> 0.6g PGA test. Figure 11 shows the shape of isolation model and LRBs failed during the extreme BDBE test of 0.6g PGA. It also describes the cross-section shape of the fully fractured LRB after the extreme dynamic test. The different colors of the scratched surface, which are friction traces due to the slip after a fracture. Similar observations were made on the cut surfaces of the deformed lead core and rubber plate. The fractured laminate occurs near the top of the LRB

laminates, which is similar to the point of maximum stress in the simulation analysis. However, as in Figure 12, displacement–time history, including the slip behavior, of the dummy mass following the test, and explains its behavior after the total break of the LRBs. The dotted line indicates the estimated time of failure initiation. Under the influence of a large input earthquake, partial failure among the LRBs by excessive shear displacement is detected at an early stage, at approximately 13 s. After a few seconds, the all of the LRBs supporting the dummy mass completely ruptured and slipped in a limited range on the table. The maximum shear displacement of the dummy mass before the break was approximately 100–110 mm (over 600% of the designed shear) and was reciprocated. The post-rupture behavior showed a slip response of approximately 70 mm in both directions on the shaking table after the center of mass moved approximately 80 mm. A detailed review of the experimental video record shows that the post-rupture behavior agrees with the response trend in Figure 11, and a small noise occurs near the point of complete break. The image in Figure 11 shows the seismic isolator LRBs supporting the dummy mass completely ruptured and moved with some rotation from the original position. It is noteworthy that, even after the LRB was completely broken, the dummy mass continued to slip within a limited range due to friction. Therefore, even if the LRB is fractured due to the occurrence of a large earthquake exceeding the DBE, there is an additional secondary seismic isolation effect due to the slip. Therefore, this should be considered in the design of isolation systems, including LRBs, superstructures, and moat margins to ensure seismic safety, and prevent potential impact with interfacing neighboring structures.



Test ID	PGA	Test condition
OPT-2C	0.6g	1-D excitation



Figure 11. Shapes of isolation system break by BDBE (PGA:0.6g).

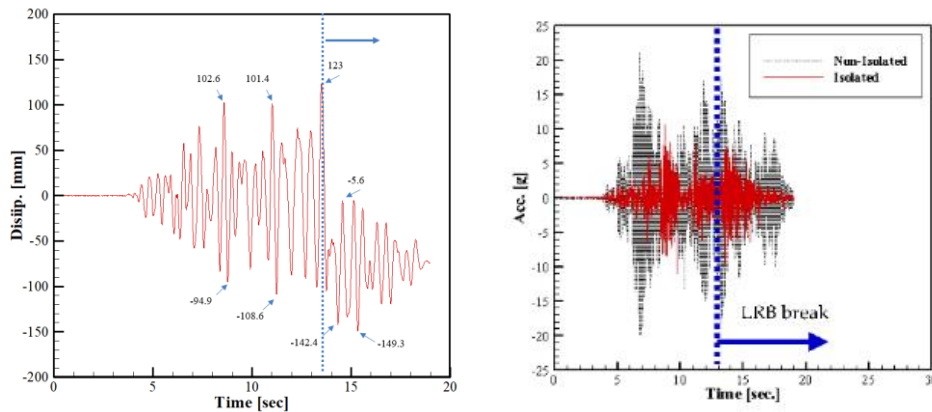


Figure 12. Response of dummy mass and 10 Hz beam structures after isolation system break (PGA:0.6g).

$$m\ddot{x} + \mu \cdot m \cdot g \cdot \text{sgn}(\dot{x}) = -m\ddot{x}_g$$

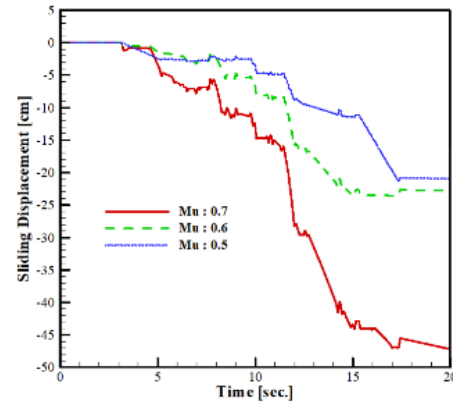
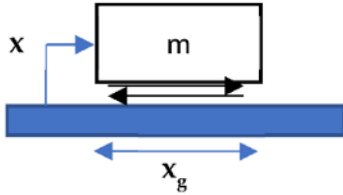


Figure 13. Simulation sliding analysis of dummy mass model

The shaking table tests confirmed that the dummy mass continued to slip within a limited range by friction, even after the LRB was completely broken. This behavior indirectly ensures the seismic safety of an isolated system using LRBs, even during BDBE. To verify the maximum displacement response resulting from the test, tests measuring the actual friction coefficient of the failed LRB and simulation slip analysis based on Equation (1) were performed for a simple block slip model and equation of motion on a friction surface shown in Figure 13. To obtain the actual friction coefficient in the case of total LRB rupture, static slip tests using inclined steel plates and dynamic tests were undertaken using a 1D shaking table. The experiments were repeated more than 10 times to ensure precision. The test averages of the static and dynamic friction coefficients  $\mu_s$  and  $\mu_d$  are 0.66 and 0.54, respectively. Figure 13 shows the displacement-time history of the sliding rigid block model for this range of friction coefficients. The maximum displacements were approximately 42, 25, and 22 cm for friction coefficients of 0.5, 0.6, and 0.7, respectively. This does not show a significant difference, considering that the actual slip displacement of 25~30 cm appeared immediately after the dummy mass was completely damaged in the shake table test for the floor response seismic input corresponding to a DBE of 0.6 g. That is, considering that the friction coefficient with the floor was estimated as 0.5~0.7 through static and dynamic friction tests, it was concluded that the slip displacement until the time when the test was stopped due to buckling of the entire seismic isolation bearing was similar to the analysis result. In general, these data determine the horizontal margin distance between the superstructure and moat wall to prevent collisions with neighboring structures during a BDBE. The study suggests that safety issues such as interference with surrounding structures can be mitigated even with a complete failure of the LRB in small facilities due to a BDBE.

## CONCLUSIONS

It was confirmed that the mechanical characteristics of LRB identified by the quasi-static tests were very similar to the results of the dynamic seismic shaking table tests. The lead plug inserted in the center of the LRB reveals a good damping function by adequately restricting the shear displacement as targeted in the LRB design. As intended in the test matrix applying sequentially from large to small level earthquakes, it was confirmed that LRB maintains seismic isolation performance against aftershocks even after experiencing the level of beyond design basis earthquakes. And it is confirmed that the developed LRB in this study shows a seismic capacity accommodating  $PGA = 0.5g$  at the 137 ft elevation of the nuclear power plant building structures. From the comparison results between the shaking table tests and the seismic analyses, it is found that the Bi-linear model or the equivalent stiffness-damping model of LRB can be used in the seismic analysis as a simple method when using well-identified stiffness and damping value of LRB. Followings are summary of conclusions.

- (1) As shown in the tests conducted in a series of tests, it was confirmed that the LRB can maintain seismic isolation performance to some degree even after an earthquake greater than the design standard occurs.
- (2) It was found that if the seismic input level used in the test was small, the seismic isolation effect was small. This is because in areas where the shear displacement of the LRB is small while the initial relative stiffness of the lead is large, the frequency shift effect of the seismic isolator become less.
- (3) As a result of repeating the same shaking table test on different LRB test bodies, almost the same results were obtained, confirming the reliability of the LRB manufacturing capability.

(4) The maximum permissible shear strain of the LRB designed and manufactured in this study is recommended to be 400%. If an input earthquake exceeding 400% shear strain is applied, it is necessary to test the shear strain limit of the LRB through additional experiments.

(5) Even when the seismic isolation bearings supporting the facility are completely broken, additional isolation by slip behavior can maintain the superstructure within the interface limit without impacting the surrounding facilities in BDBE.

(6) The small-sized LRB studied in the paper can be a good option among seismic isolation devices for the seismic enhancement of the selective safety-related equipment of operating nuclear plants.

## **ACKNOWLEDGMENTS**

This study was funded by the Ministry of Trade, Industry and Energy through KETEP (Korea Institute of Energy Technology Evaluation Planning). (No. 20224B10200080)

## **REFERENCES**

- [1] Koo, G.-H.; Shin, T.-M.; Ma, S.-J. (2021), "Shaking Table Tests of Lead Inserted Small-Sized Laminated Rubber Bearing for Nuclear Component Seismic Isolation". *Appl. Sci.*, 11, 4431
- [2] Koo, G.-H.; Jung, J.-Y.; Lee, J.-H.; Shin, T.-M.; Park, J.-Y. (2020), "Development of Small-Sized Lead Inserted Laminated Rubber Bearing for Nuclear Component Seismic Isolation." *Energies*, 13, 3193.
- [3] Cho, S.G.; Chang, S.K.; Sung, D.Y. (2020), "Application of tuned mass damper to mitigation of the seismic responses of electrical equipment in nuclear power plants." *Energies*, 13, 427.
- [4] Kostarev, V.; Petrenko, A.; Vasilev, P.A. (2020), "New Method for Essential Reduction of Seismic and External Loads on NPP's Structures, Systems and Components." In *Proceedings of the 17th International Conference on SMiRT, Prague, Czech Republic, 17–22 August; Volume K13-1.*
- [5] Koo, G.H.; Lee, J.H.; Yoo, B.; Ohtori, Y. (1999), "Evaluation of Laminated Rubber Bearing for Seismic Isolation Using Modified Macro- Model with Parameter Equations of Instantaneous Apparent Shear Modulus." *Eng. Struct.*, 21, 594–602
- [6] Eidinger, J.K.; Tajirian, F.F.; Kircher, C.A.; Vaidya, N.; Constantinou, M.; Kelly, J.M.; Ovardia, D.; Seidensticker, R. (1989), "Base Isolation for Nuclear Power and Nuclear Material Facilities." *Proceedings of the Second DOE Natural Phenomena Hazards Mitigation Conference, Lawrence Livermore National Lab, Knoxville, TN, USA, 3–5 October; pp. 46–57.*
- [7] Fujita, T.; Fujita, S.; Suzuki, S.; Yoshizawa, T. (1987), "Experimental Study of Laminated Rubber Bearings for Earthquake Isolation of Buildings." *Trans. Jpn. Soc. Mech. Eng.*, 53, 71–76.
- [8] Carlos, M.V.; Tianjian, J. (2015), "Seismic protection technology for nuclear power plants: A systematic review." *J. Nucl. Sci. Technol.*, 52, 607–632.
- [9] *Seismic Isolation Systems for Nuclear Installations; (2020), IAEA-TECDOC-1905; IAEA: Vienna, Austria.*
- [10] ISO 22762-1(2010), "Elastomeric Seismic-Protection Isolators—Part 1: Test Methods." *International Standardization Organization, Geneva, Switzerland.*
- [11] Kubo, T.; Yamamoto, T.; Saro, K.; Jimbo, M.; Imaoka, T.; Umeki, Y. (2014), "A Seismic Design of Nuclear Reactor Building Structures Applying Seismic Isolation System in A High Seismicity Region—A Feasibility Case Study In JAPAN." *Nucl. Eng. Technol.*, 46, 716.
- [12] Sato, N.; Watanabe, Y.; Kato, A.; Ohba, M.; Fukushima, Y.; Iizuka, M.; Yoshikawa, K.; Umeki, K.; Suhara, J.; Murazumi, Y.; et al. (2000), "Shaking Table Test and Analysis on Ultimate Characteristics of the Lead Rubber Bearing for Base Isolated FBR Plant." In *Proceedings of the 12th World Conference on Earthquake Engineering, Auckland, New Zealand, 30 January–4 February.*
- [13] Moteki, M.; Kawai, N.; Ishida, K.; Yabana, S.; Nojima, O. (1992), "Shaking table test on ultimate behavior of seismic isolation system, Part 1: Outline of the test and response of superstructure." In *Proceedings of the 10th World Conference on Earthquake Engineering; Madrid, Spain, 19–24 July, pp. 2271–2276.*
- [14] Sato, N.; Kato, A.; Fukushima, Y.; Iizuka, M. (2002), "Shaking table tests on failure characteristics of base isolation system for a DFBR plant." *Nucl. Eng. Des.*, 212, 293–305.
- [15] *Design Response Spectra for Seismic Design of Nuclear Power Plants (1973), Regulatory Guide 1.60; Nuclear Regulatory Commission: Rockville, MD, USA*
- [16] ANSYS. (2020) *Mechanical APDL Release 20.*; ANSYS, Inc., Canonsburg, PA, USA. <http://www.ansys.com/>